NUCL SCI TECH (2021) 32:53
https://doi.org/10.1007/s41365-021-00889-9

First proof-of-principle experiment with the post-accelerated isotope separator on-line beam at BRIF: measurement of the angular distribution of ^{23}Na + ^{40}Ca elastic scattering

Wei Nan[1] · Bing Guo[1] · Cheng-Jian Lin[1,2] · Lei Yang[1] · Dong-Xi Wang[1] · Yang-Ping Shen[1] · Bing Tang[1] · Bao-Qun Cui[1] · Tao Ge[1] · Yin-Long Lyu[1] · Hui-Ming Jia[1] · Yun-Ju Li[1] · Chen Chen[1] · Li-Hua Chen[1] · Qi-Wen Fan[1] · Xin-Yue Li[3] · Gang Lian[1] · Jian-Cheng Liu[1] · Tian-Peng Luo[1] · Nan-Ru Ma[1] · Rui-Gang Ma[1] · Xie Ma[1] · Ying-Jun Ma[1] · Wei-Ke Nan[1] · Dan-Yang Pang[4,5] · You-Bao Wang[1] · Pei-Wei Wen[1] · Feng Yang[1] · Yong-Jin Yao[1,4] · Sheng Zeng[1] · Hao Zhang[1] · Fu-Peng Zhong[1,2] · Shan-Hao Zhong[1,2] · Zhi-Hong Li[1] · Tian-Jue Zhang[1] · Wei-Ping Liu[1] · BRIF Collaboration

Received: 21 April 2021 / Revised: 21 April 2021 / Accepted: 29 April 2021 / Published online: 24 May 2021

Abstract The reaction dynamics of exotic nuclei near the drip line is one of the main research topics of current interest. Elastic scattering is a useful probe for investigating the size and surface diffuseness of exotic nuclei. The development of rare isotope accelerators offers opportunities for such studies. To date, many relevant measurements have been performed at accelerators using the projectile fragmentation technique, while the measurements at accelerators using isotope separator on-line (ISOL) systems are still quite scarce. In this work, we present the first proof-of-principle experiment with a post-accelerated ISOL beam at the Beijing Radioactive Ion Beam Facility (BRIF) by measuring the angular distribution of elastic scattering for the stable nucleus ^{23}Na from the doubly magic nucleus ^{40}Ca at energies above the Coulomb barrier. The angular distribution measured by a silicon strip detector array in a scattering chamber using the ISOL beam at BRIF is in good agreement with that measured by the high-precision Q3D magnetic spectrograph using the non-ISOL beam at nearly the same energy. This work provides useful background for making BRIF a powerful tool for the investigation of the reaction dynamics of exotic nuclei.

Keywords BRIF · Exotic nuclei · Elastic scattering · Angular distribution

1 Introduction

Light loosely bound nuclei near the drip line are characterized by very low nucleon binding energies, typically one order of magnitude smaller than those for their stable counterparts located along the β-stability valley. These nuclei can exhibit exotic properties, such as a halo structure. The reaction dynamics of light exotic nuclei near the drip line is one of the main research topics of current

This work was supported by the National Natural Science Foundation of China (Nos. 11490561, 11635015, 11961141003, 11805280, 11975316, 12075045, 12005304, U1867212, and U1867214), the National Key Research and Development Project (Nos. 2016YFA0400502 and 2018YFA0404404), the Continuous Basic Scientific Research Project (No. WDJC-2019-13), and the Leading Innovation Project (Nos. LC192209000701 and LC202309000201).

✉ Bing Guo
guobing@ciae.ac.cn

✉ Cheng-Jian Lin
cjlin@ciae.ac.cn

✉ Wei-Ping Liu
wpliu@ciae.ac.cn

[1] China Institute of Atomic Energy (CIAE), P.O. Box 275(10), Beijing 102413, China

[2] Department of Physics, Guangxi Normal University, Guilin 541004, China

[3] College of Nuclear Science and Technology, Beijing Normal University, Beijing 100875, China

[4] School of Physics, Beihang University, Beijing 100191, China

[5] Key Laboratory of Advanced Nuclear Materials and Physics, Beihang University, Beijing 100191, China

interest and has attracted considerable interest in the low-energy nuclear physics community [1–3]. Elastic scattering is a useful probe for investigating the size and surface diffuseness of exotic nuclei by comparing the similarities and differences in the angular distributions of the reactions induced by loosely bound and tightly bound nuclei [4].

To date, several measurements have been made of the elastic-scattering angular distributions of neutron-rich nuclei, such as the 2*n*-halo nuclei ^{6}He [5] and ^{11}Li [6], neutron skin nucleus ^{8}He [7, 8], ^{8}Li [9], and the 1*n*-halo nucleus ^{11}Be [10–12]. In recent years, the elastic scattering of proton-rich nuclei has also been investigated (e.g., ^{7}Be, ^{8}B, ^{9}C + Pb [4, 13, 14], ^{17}F + ^{12}C and ^{14}N [15], ^{17}F + ^{58}Ni [16], ^{17}F + ^{89}Y [17], and ^{17}F + ^{208}Pb [18, 19]). These experiments have greatly deepened our understanding of the reaction dynamics and their interplay with the exotic structure of weakly bound nuclei. However, more investigations are needed.

The development of rare isotope accelerators offers opportunities to explore the structure of unstable exotic nuclei. There are two rare complementary isotope accelerators in China. One is the Radioactive Ion Beam Line in Lanzhou (RIBLL) [20] using the projectile fragmentation (PF) technique, which was established by the Institute of Modern Physics, Chinese Academy of Sciences. Since the delivery of the first beam in 1997, a series of experiments have been conducted for the study of, for example, the clustering structure in neutron-rich nuclei [21, 22], two-proton emission in proton-rich nuclei [23, 24], and revalidation of the isobaric multiplet mass equation [25]. In addition, the elastic-scattering angular distributions of a few proton-rich nuclei [4, 13, 17] and the 1*n*-halo nucleus ^{11}Be [12] have been measured using silicon detector arrays [26, 27] at RIBLL. The other accelerator is the Beijing Radioactive Ion Beam Facility (BRIF) [28, 29] using the isotope separator on-line (ISOL) technique, which was established by the China Institute of Atomic Energy. BRIF consists of a 100-MeV 200-μA compact proton cyclotron [30], an ISOL system with a mass resolution of 20,000 [31], and a 13-MV tandem accelerator for post-acceleration. BRIF was commissioned in 2015 and successfully produced a few unstable ion beams such as ^{20,21,22}Na and ^{37,38}K. Recently, the exotic β–γ–α decay mode was directly observed for the first time with a pure ^{20}Na ISOL beam at BRIF [32].

BRIF is a potential high-precision facility for investigating the nuclear reaction dynamics of unstable nuclei, as it can deliver almost pure unstable ion beams. However, an experiment with a post-accelerated ISOL beam at BRIF has not been performed to date. Therefore, a proof-of-principle experiment with a post-accelerated stable ^{23}Na beam is highly desirable. For this purpose, the angular distribution of ^{23}Na + ^{40}Ca elastic scattering was measured using two techniques. One is based on a silicon detector array with a post-accelerated ^{23}Na beam using the ISOL technique at BRIF (ISOL beam); the other is based on a high-precision Q3D spectrograph with the ^{23}Na beam directly from the traditional negative-ion source and accelerated by the HI-13 tandem accelerator (non-ISOL beam). The excellent consistency of these two results demonstrates that BRIF can be a powerful tool for investigating the reaction dynamics of exotic nuclei.

2 Experimental setup and procedure

The experiment with the post-accelerated ISOL beam was performed at BRIF. First, a non-ISOL ^{23}Na beam directly from an ion source was accelerated by the HI-13 tandem accelerator as the pilot beam and transported to the R60 scattering target chamber to determine the beam optics. Second, the proton cyclotron served as the driving accelerator. The ^{23}Na beam was then produced with a 100-MeV 10-eμA proton beam from the cyclotron bombarding the MgO target. Reaction products diffusing out of the thick target were ionized by an ion source and separated by a two-stage ISOL system for subsequent post-acceleration. Finally, the ISOL ^{23}Na beam was accelerated by using the HI-13 tandem accelerator and transported to the R60 scattering target chamber for the angular distribution measurement with the same optical systems as used for the pilot beam. The energy and the current of the ISOL ^{23}Na beam were 83.25 MeV and 0.5 enA, respectively.

The setup of the target chamber is illustrated in Fig. 1. Two micro-channel plates (MCPs), which can present a fast timing signal, were used to measure the time of flight (TOF) of the beam. A quadrant silicon detector (QSD) with

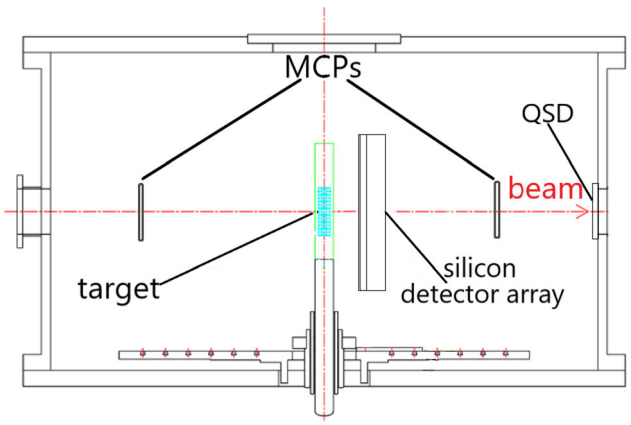

Fig. 1 (Color online) Experimental setup in the target chamber. The two MCPs and the QSD were used to identify the beam. A silicon detector array was used to detect emitted particles

a thickness of 1000 μm, which was placed at the end of the target chamber, was used to measure the total energy of the beam. The ISOL beam from BRIF can be confirmed by a combination of the TOF and energy. After the development of the ^{23}Na beam was confirmed, the upstream MCP and QSD were removed to avoid interference with the measurement of the angular distribution, while the downstream MCP was left to monitor the beam. The target was made by evaporation of natural CaF_2 with a thickness of 118 μg/cm^2 on a 200 μg/cm^2 thick Au foil. The silicon detector array was placed 10 cm downstream of the target. The detector array consists of four detector telescopes, as shown in Fig. 2. The first and second layers of each telescope are two single-sided silicon strip detectors (SSSDs) with thicknesses of 20 and 300 μm, respectively. Each SSSD has a typical energy resolution of 0.3% and has 16 strips with a width of 3 mm, spaced 0.1 mm apart. These two SSSDs were placed in the horizontal and vertical directions, respectively. The third layer is a QSD with a thickness of 1000 μm and an area of 50×50 mm^2 for potential light reaction products such as protons and α particles. Such a configuration can identify reaction products, including light and heavy ions. The angular coverage range of the present detector array in the laboratory system ranges from 10.2° to 39.6°, as shown in Fig. 3.

In this experiment, the energy of the ^{23}Na beam at the center of the target was 82.8 MeV. The scattered ^{23}Na ions were detected in the first two layers of the telescope. The

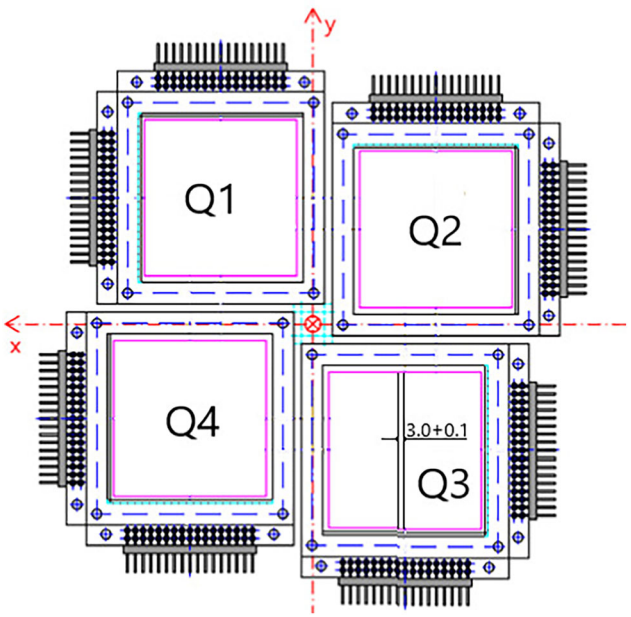

Fig. 2 (Color online) Setup of the silicon detector array. The detector array consists of four detector telescopes. Each detector telescope contains three layers of silicon detectors with thicknesses of 20, 300, and 1000 μm, respectively. See the text for further details

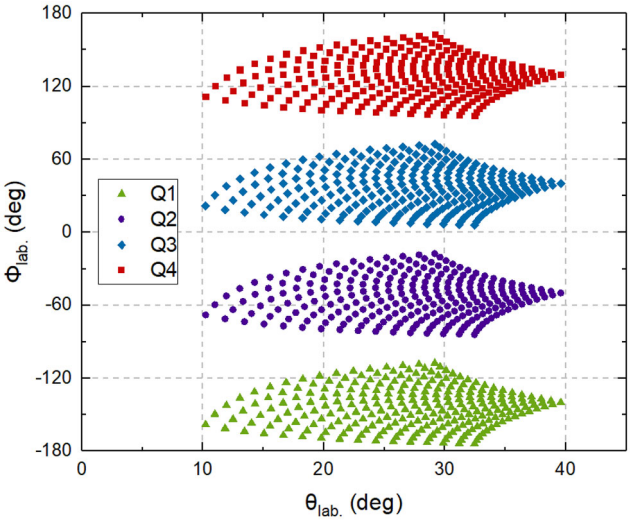

Fig. 3 (Color online) Angular coverage of the detector array. θ and ϕ are the angles used in the spherical coordinate system. The array covers the scattering angle θ, ranging from 10.2° to 39.6°

20-μm-thick SSSD was used for the measurement of energy loss ΔE, while a 300-μm-thick SSSD was used to measure the residual energy E_r. The experimental spectra of the scattered ^{23}Na particles from ^{40}Ca and ^{197}Au are shown in Fig. 4. Both the two-dimensional spectrum of energy loss versus the total energy and the one-dimensional spectrum of the total energy are presented. The ^{23}Na particles from ^{40}Ca can be clearly distinguished from those from ^{197}Au.

To verify the ISOL-based technique at BRIF, the same angular distribution was also measured with a well-developed technique using a high-precision Q3D spectrograph with the non-ISOL ^{23}Na beam directly from the traditional negative-ion source and accelerated by the HI-13 tandem accelerator at the China Institute of Atomic Energy. The experimental setup and procedures were identical to those reported in our previous work [33, 34]. The experimental target was made by evaporation of natural CaF_2 with a thickness of 18 μg/cm^2 on a 30 μg/cm^2 thick Au foil. In this experiment, the energy of the ^{23}Na beam was 84 MeV, and its energy at the center of the target was 83.9 MeV (which was almost the same as the measurement at BRIF).

3 Data analysis and results

The differential cross section of a reaction can be expressed as

$$\sigma = \frac{N}{IN_S\Omega}, \quad (1)$$

where N and I represent the numbers of emitted ions and

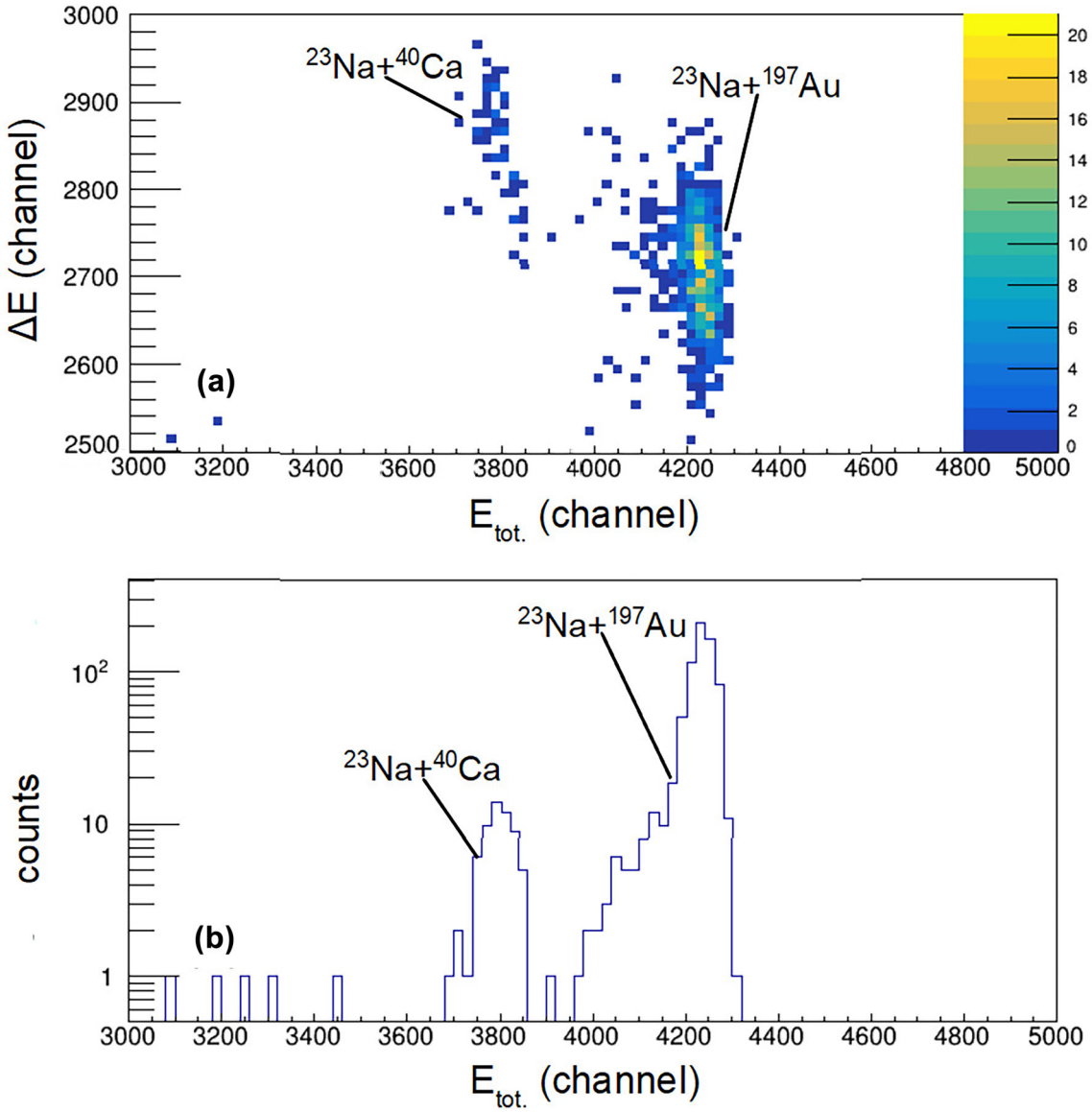

Fig. 4 (Color online) Energy spectra of the scattered ^{23}Na particles from ^{40}Ca and ^{197}Au. **a** Two-dimensional spectrum of energy loss ΔE versus total energy E_{tot}. **b** One-dimensional spectrum of total energy

incident ions, respectively, N_{s} denotes the number of target atoms per unit area, and Ω represents the solid angle. In the present work, we used a relative measurement method to reduce the uncertainties from the solid angle and beam intensity. The cross section of ^{23}Na + ^{197}Au elastic scattering at the present energy is equal to the Rutherford cross section; therefore, the ratio of the measured ^{23}Na + ^{40}Ca elastic-scattering cross section to the corresponding Rutherford cross section can be calculated by using

$$\mathrm{d}\sigma/\mathrm{d}\sigma_{\mathrm{r}}^{\mathrm{Ca}} = \frac{N^{\mathrm{Ca}} \times N_{\mathrm{S}}^{\mathrm{Au}} \times \mathrm{d}\sigma_{\mathrm{r}}^{\mathrm{Au}}}{N^{\mathrm{Au}} \times N_{\mathrm{S}}^{\mathrm{Ca}} \times \mathrm{d}\sigma_{\mathrm{r}}^{\mathrm{Ca}}}, \tag{2}$$

where N^{Ca} and N^{Au} are the numbers of the scattered ^{23}Na ions from ^{40}Ca and ^{197}Au, respectively; $N_{\mathrm{S}}^{\mathrm{Ca}}$ and $N_{\mathrm{S}}^{\mathrm{Au}}$ are the numbers of Ca and Au atoms per unit area of the target, respectively; and $\mathrm{d}\sigma_{\mathrm{r}}^{\mathrm{Ca}}$ and $\mathrm{d}\sigma_{\mathrm{r}}^{\mathrm{Au}}$ are the Rutherford differential cross sections of ^{23}Na + ^{40}Ca and ^{23}Na + ^{197}Au, respectively. It can be seen that the uncertainties from the solid angle and beam intensity can be removed through the present relative measurement method.

In Fig. 5, we show the experimental angular distribution of ^{23}Na + ^{40}Ca elastic scattering with the ISOL-based technique at BRIF and a well-developed technique at a high-precision Q3D spectrograph, together with the optical model calculations with the single-folding potential [35]. These two experimental results were in good agreement. This presents strong evidence that BRIF can be used for such measurements.

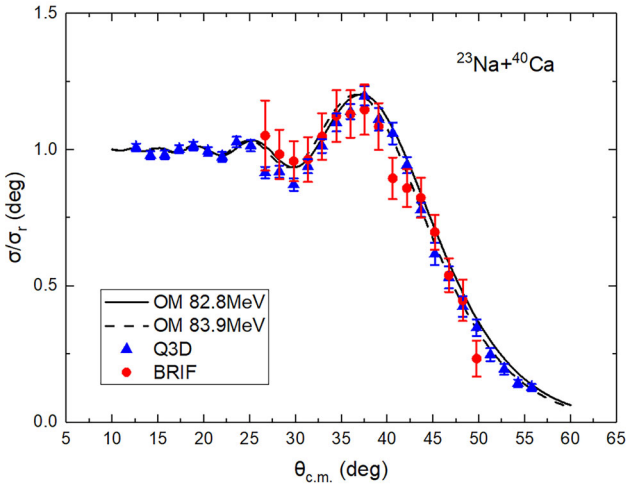

Fig. 5 (Color online) Angular distribution of ^{23}Na + ^{40}Ca elastic scattering. The red points are the results obtained using the ISOL-based technique at BRIF, while the blue points represent those obtained with the well-developed technique using a high-precision Q3D spectrograph. The solid and dashed curves stand for the optical model (OM) calculations at 82.8 and 83.9 MeV, respectively

4 Conclusion and perspective

In this work, we performed the first proof-of-principle experiment with a post-accelerated ^{23}Na beam using the ISOL technique at BRIF (ISOL beam) by measuring the angular distribution of ^{23}Na + ^{40}Ca elastic scattering. In addition, we measured the same angular distribution with a well-developed technique using a high-precision Q3D spectrograph with a ^{23}Na beam from the HI-13 tandem accelerator (non-ISOL beam). These two results are in excellent agreement, demonstrating that BRIF can be a powerful tool for future investigation of the reaction dynamics of exotic nuclei.

To the best of our knowledge, there are no elastic-scattering data for unstable sodium isotopes ^{20,21,22}Na on the doubly magic nucleus ^{40}Ca. To explore the exotic properties of these unstable sodium isotopes, we plan to measure the angular distribution of ^{21,22}Na + ^{40}Ca elastic scattering at BRIF using the same technique described in this work in the near future.

Author Contributions All authors contributed to the study conception and design. Experiment was carried out by Wei Nan, Cheng-Jian Lin, Lei Yang, Dong-Xi Wang, Yang-Ping Shen, Hui-Ming Jia, Yun-Ju Li, and Xin-Yue Li. Targets were made by Qi-Wen Fan. Data analysis was performed by Wei Nan, Bing Guo, Cheng-Jian Lin, Yang-Ping Shen, Dan-Yang Pang, and Wei-Ping Liu. The ISOL beam was developed by Bing Tang, Bao-Qun Cui, Tao Ge, Yin-Long Lyu, Li-Hua Chen, Jian-Cheng Liu, Rui-Gang Ma, Xie Ma, Ying-Jun Ma, and Tian-Jue Zhang. The first draft of the manuscript was written by Wei Nan and all authors commented on previous versions of the manuscript. All authors read and approved the final manuscript.

References

1. N. Keeleya, R. Raabe, N. Alamanos et al., Fusion and direct reactions of halo nuclei at energies around the Coulomb barrier. Prog. Part. Nucl. Phys. **59**, 579 (2007). https://doi.org/10.1016/j.ppnp.2007.02.002
2. N. Keeleya, N. Alamanos, K.W. Kemper et al., Elastic scattering and reactions of light exotic beams. Prog. Part. Nucl. Phys. **63**, 396 (2009). https://doi.org/10.1016/j.ppnp.2009.05.003
3. B.B. Back, H. Esbensen, C.L. Jiang et al., Recent developments in heavy-ion fusion reactions. Rev. Mod. Phys. **86**, 317 (2014). https://doi.org/10.1103/RevModPhys.86.317
4. Y.Y. Yang, J.S. Wang, Q. Wang et al., Elastic scattering of the proton drip-line nucleus ^{8}B off a ^{nat}Pb target at 170.3 MeV. Phys. Rev. C **87**, 044613 (2013). https://doi.org/10.1103/PhysRevC.87.044613
5. L. Acosta, A.M. Sanchez-Benitez, M.E. Gomez et al., Elastic scattering and α-particle production in ^{6}He+^{208}Pb collisions at 22 MeV. Phys. Rev. C **84**, 044604 (2011). https://doi.org/10.1103/PhysRevC.84.044604
6. M. Cubero, J.P. Fernandez-Garcia, M. Rodriguez-Gallardo et al., Do Halo Nuclei Follow Rutherford Elastic Scattering at Energies Below the Barrier? The Case of ^{11}Li. Phys. Rev. Lett. **109**, 262701 (2012). https://doi.org/10.1103/PhysRevLett.109.262701
7. A. Lemasson, A. Shrivastava, A. Navin et al., Modern Rutherford experiment: Tunneling of the most neutron-rich nucleus. Phys. Rev. Lett. **103**, 232701 (2009). https://doi.org/10.1103/PhysRevLett.103.232701
8. G. Marquínez-Durán, I. Martel, A.M. Sanchez-Benitez et al., Precise measurement of near-barrier ^{8}He+^{208}Pb elastic scattering: comparison with ^{6}He. Phys. Rev. C **94**, 064618 (2016). https://doi.org/10.1103/PhysRevC.94.064618
9. K.J. Cook, I.P. Carter, E.C. Simpson et al., Interplay of charge clustering and weak binding in reactions of ^{8}Li. Phys. Rev. C **97**, 021601(R) (2018). https://doi.org/10.1103/PhysRevC.97.021601
10. A. Di Pietro, G. Randisi, V. Scuderi et al., Elastic scattering and reaction mechanisms of the halo nucleus ^{11}Be around the Coulomb barrier. Phys. Rev. Lett. **105**, 022701 (2010). https://doi.org/10.1103/PhysRevLett.105.022701
11. V. Pesudo, M.J.G. Borge, A.M. Moro et al., Scattering of the halo nucleus ^{11}Be on ^{197}Au at energies around the Coulomb barrier. Phys. Rev. Lett. **118**, 152502 (2017). https://doi.org/10.1103/physrevlett.118.152502
12. F.F. Duan, Y.Y. Yang, K. Wang et al., Scattering of the halo nucleus ^{11}Be from a lead target at 3.5 times the Coulomb barrier energy. Phys. Lett. B **811**, 135942 (2020). https://doi.org/10.1016/j.physletb.2020.135942
13. Y.Y. Yang, X. Liu, D.Y. Pang et al., Elastic scattering of the proton drip line nuclei ^{7}Be, ^{8}B, and ^{9}C on a lead target at energies around three times the Coulomb barriers. Phys. Rev. C **98**, 044608 (2018). https://doi.org/10.1103/PhysRevC.98.044608
14. M. Mazzocco, N. Keeley, A. Boiano et al., Elastic scattering for the ^{8}B and ^{7}Be+^{208}Pb systems at near-Coulomb barrier energies. Phys. Rev. C **100**, 024602 (2019). https://doi.org/10.1103/PhysRevC.100.024602
15. J.C. Blackmon, F. Carstoiu, L. Trache et al., Elastic scattering of the proton drip-line nucleus ^{17}F. Phys. Rev. C **72**, 034606 (2005). https://doi.org/10.1103/PhysRevC.72.034606
16. L. Yang, C.J. Lin, H. Yamaguchi et al., Insight into the reaction dynamics of proton drip-line nuclear system ^{17}F + ^{58}Ni at near-barrier energies. Phys. Lett. B **813**, 136045 (2021). https://doi.org/10.1016/j.physletb.2020.136045
17. G.L. Zhang, G.X. Zhang, C.J. Lin et al., Angular distribution of elastic scattering induced by ^{17}F on medium-mass target nuclei at

energies near the Coulomb barrier. Phys. Rev. C **97**, 044618 (2018). https://doi.org/10.1103/PhysRevC.97.044618
18. J.F. Liang, J.R. Beene, H. Esbensen et al., Elastic scattering and breakup of ^{17}F at 10 MeV/nucleon. Phys. Rev. C **65**, 051603(R) (2002). https://doi.org/10.1103/PhysRevC.65.051603
19. M. Romoli, E. Vardaci, M. Di Pietro et al., Measurements of ^{17}F scattering by ^{208}Pb with a new type of large solid angle detector array. Phys. Rev. C **69**, 064614 (2004). https://doi.org/10.1103/PhysRevC.69.064614
20. Z. Sun, W.-L. Zhan, Z.-Y. Guo et al., The radioactive ion beam line in Lanzhou. Nucl. Instrum. Methods Phys. Res. Sect. A **503**, 496 (2003). https://doi.org/10.1016/S0168-9002(03)01005-2
21. Z.H. Yang, Y.L. Ye, Z.H. Li et al., Observation of enhanced monopole strength and clustering in ^{12}Be. Phys. Rev. Lett. **112**, 162501 (2014). https://doi.org/10.1103/PhysRevLett.112.162501
22. Y. Liu, Y.L. Ye, J.L. Lou et al., Positive-parity linear-chain molecular band in ^{16}C. Phys. Rev. Lett. **124**, 192501 (2020). https://doi.org/10.1103/PhysRevLett.124.192501
23. X.X. Xu, C.J. Lin, L.J. Sun et al., Observation of β-delayed two-proton emission in the decay of ^{22}Si. Phys. Lett. B **766**, 312 (2017). https://doi.org/10.1016/j.physletb.2017.01.028
24. Y.T. Wang, D.Q. Fang, K. Wang et al., Observation of β-delayed ^{2}He emission from the proton-rich nucleus ^{22}Al. Phys. Lett. B **784**, 12 (2018). https://doi.org/10.1016/j.physletb.2018.07.034
25. J. Su, W.P. Liu, N.T. Zhang et al., Revalidation of the isobaric multiplet mass equation at A=53, T=3/2. Phys. Lett. B **756**, 323 (2016). https://doi.org/10.1016/j.physletb.2016.03.024
26. G.L. Zhang, Y.J. Yao, G.X. Zhang et al., A detector setup for the measurement of angular distribution of heavy-ion elastic scattering with low energy on RIBLL. Nucl. Sci. Tech. **28**, 104 (2017). https://doi.org/10.1007/s41365-017-0249-0
27. F.F. Duan, Y.Y. Yang, B.T. Hu et al., Silicon detector array for radioactive beam experiments at HIRFL-RIBLL. Nucl. Sci. Tech. **29**, 165 (2018). https://doi.org/10.1007/s41365-018-0499-5
28. W.P. Liu, Z.H. Li, X.X. Bai et al., Current progress of nuclear astrophysics study and BRNBF at CIAE. Nucl. Instrum. Methods Phys. Res. Sect. B **204**, 62 (2003). https://doi.org/10.1016/S0168-583X(02)01892-X
29. B. Guo, W.P. Liu, Beijing radioactive ion beam facility and basic nuclear physics research prospects (in Chinese). Chin. Sci. Bull. **60**, 1820–1827 (2015). https://doi.org/10.1360/N972014-01209
30. T.J. Zhang, Z.G. Li, Z.G. Yin et al., Design and construction status of CYCIAE-100, a 100 MeV H^- cyclotron for RIB production. Nucl. Instrum. Methods Phys. Res. Sect. B **266**, 4117 (2008). https://doi.org/10.1016/j.nimb.2008.05.021
31. B.Q. Cui, Z.H. Peng, Y.J. Ma et al., Status of Beijing radioactive ion beam facility. Res. Sect. B **266**, 4113 (2008). https://doi.org/10.1016/j.nimb.2008.05.154
32. Y.B. Wang, J. Su, Z.Y. Han et al., Direct observation of the exotic β-γ-α decay mode in the T_z = 1 nucleus ^{20}Na. Phys. Rev. C **103**, L011301 (2021). https://doi.org/10.1103/PhysRevC.103.L011301
33. Y.P. Shen, B. Guo, T.L. Ma, First experimental constraint of the spectroscopic amplitudes for the α-cluster in the ^{11}B ground state. Phys. Lett. B **797**, 134820 (2019). https://doi.org/10.1016/j.physletb.2019.134820
34. Y.P. Shen, B. Guo, R.J. de Boer, Constraining the External Capture to the ^{16}O Ground State and the E2 S Factor of the ^{12}C(α, γ)^{16}O Reaction. Phys. Rev. Lett. **124**, 162701 (2020). https://doi.org/10.1103/PhysRevLett.124.162701
35. D.Y. Pang, Y.L. Ye, F.R. Xu, Application of the Bruyeres Jeukenne–Lejeune–Mahaux model potential to composite nuclei with a single-folding approach. Phys. Rev. C **83**, 064619 (2011). https://doi.org/10.1103/PhysRevC.83.064619